



Novel beer bitterness measurement instrument using optical fiber sensor

Renato Luiz Faraco Filho ^{a,*}, Felipe Oliveira Barino ^a, João Victor Calderano ^a, Deivid Campos ^b, Italo Fernandes Valle Alvarenga ^a, André William Paviani Manhas ^c, Alexandre Bessa dos Santos ^a

^a Department of Circuits, Federal University of Juiz de Fora, Juiz de Fora, Minas Gerais, 36036-900, Brazil

^b Department of Computational and Applied Mechanics, Federal University of Juiz de Fora, Juiz de Fora, Minas Gerais, 36036-900, Brazil

^c Ambev, Jacareí, São Paulo, 12334-480, Brazil

ARTICLE INFO

Keywords:

Optical fiber sensor

Food quality

Bitterness

Taste sensing

ABSTRACT

This paper presents a novel optical fiber sensor for measuring the bitterness of beer samples. The sensor is based on a Mach-Zehnder interferometer (MZI) composed of two long-period fiber gratings (LPFGs). The sensor exploits the sensitivity of the LPFGs to the refractive index of the surrounding medium, which varies according to the concentration of iso- α -acids that cause bitterness in beer. The sensor uses a two-point online self-calibrating procedure to estimate the bitterness of unknown samples by comparison with reference samples of known bitterness. The sensor performance was evaluated in both laboratory and factory settings, showing good repeatability, reproducibility, and low bias. The proposed sensor offers a fast, simple, and low-cost alternative to the conventional method of measuring beer bitterness based on UV spectroscopy. The sensor can be integrated into the Industry 4.0 framework to improve the quality and consistency of beer production.

1. Introduction

Beer stands as one of the earliest and most revered beverages across the globe with a millennia-long history. There is evidence suggesting that beer originated in ancient Mesopotamia around 4000 BC (Damerow, 2012). Over the centuries, beer has played a significant role with substantial influence in social, economic, and cultural spheres within diverse societies.

Over the centuries, manufacturing processes have undergone significant transformations. The advent of industrialization and large-scale production has caused several fundamental shifts. Currently, a new industrial revolution is unfolding, facilitated by the emergence of artificial intelligence and the capability to gather and analyze vast amounts of data. Named as Industry 4.0, this revolution integrates the data collection potential of the Internet of Things (IoT) with the computational capabilities of machine learning and cloud computing within manufacturing setups. The pivotal advantages brought by this revolution incorporate intelligent manufacturing, instantaneous automated decision-making, predictive maintenance, traceability, increased automation, and enhanced quality monitoring (Cañas et al., 2021; Lasi et al., 2014; Zhou et al., 2015).

The food industry was one of the most-growing markets. Its vitality pushes quality control to the limit. However, despite the recent context of the Industry 4.0, food quality control has not evolved as fast as some areas. Conventional methods for assessing quality are often

arduous, time-consuming, and invasive. However, the technologies associated with Industry 4.0 offer promising solutions to overcome these challenges (Hassoun et al., 2023a,b). Data-driven solutions can be implemented through the whole manufacturing process and can help solve production problems involving climate change, resource selection, recycling, aging, and sensory evaluation for example Esmaeily et al. (2024).

Naturally, the beer industry has been implementing Industry 4.0 technologies to improve the quality and consistency of its products. Among these advancements, the use of sensors has emerged as a transformative innovation in beer production (Benadouda et al., 2023; Viejo and Fuentes, 2020). Sugar and ethanol concentration measurements and detection of contaminants (Jaywant et al., 2022; Xu et al., 2020; Tsai et al., 2007). Other research proposes the use of data-driven techniques coupled with data collection methods such as e-nose and e-tongue for sample discrimination and characterization of beer parameters (Blanco et al., 2015; Shi et al., 2019). However, most of the research efforts, until 2023, for sensing in beer were focused on detecting toxins and ethanol (Benadouda et al., 2023). Consequently, practical plug-and-play sensors have not been proposed for some parameters.

There is no doubt that beer taste is a crucial factor in its popularity and determining its quality. One of the key components that contribute to the taste of beer is its bitterness. Bitterness is caused by the presence

* Corresponding author.

E-mail address: renato.luiz@engenharia.ufjf.br (R.L. Faraco Filho).

of iso- α -acids in beer, which are produced during the brewing process. Measuring the bitterness of beer is important for ensuring that the beer has a consistent taste and quality.

For instance, the bitterness of beer demands the use of arduous and time-consuming methodology. Presently, measuring beer bitterness involves transporting a beer sample to a laboratory where its absorbance of ultraviolet light is analyzed and scaled to the International Bitterness Unit (IBU). The process involves extracting an acidified beer solution into isoctane, followed by measuring absorbance at 275 nm, as this wavelength offers the highest absorbance for elements contributing to beer bitterness (Bishop, 1964; Hunter and Domkowski, 2018).

Usually, this laboratory process involves 4 steps: preparation of chemical solutions, beer sampling, ultraviolet (UV) spectroscopy, and result analysis. Each step must be done carefully and requires safety precautions. Chemical solutions should be prepared in a dedicated laboratory, and precautions should be taken during beer sampling to minimize foam formation, which should be promptly removed if it occurs. Sample analysis requires temperature control and the use of laboratory equipment such as centrifuges, spectrophotometers, and shakers.

In this paper, we propose a novel method to measure the bitterness of beers by applying optical fiber sensors to measure the variation of the refractive index of different beers samples and correlate it to their IBU. This kind of sensor has some advantages, such as immunity to electromagnetic and radio frequency interferences, high sensitivity, small size, lightweight and wide dynamic range (Filho et al., 2021; Roriz et al., 2020). Our method employs a Mach-Zehnder interferometer (MZI) manufactured from a pair of long period fiber gratings (LPFGs) that was produced by inducing electric arcs periodically in the optical fiber. Besides the advantages of the optical fiber sensors, this interferometer has some particular characteristics, offering high sensitivity and precision, providing a real-time measurement.

Through this investigation, we found that our novel method presents measurements as precise as the previous ones, despite the precision offered by traditional methods. However, our measurements are significantly quicker, require a smaller setup, and can be controlled remotely due to the low attenuation of optical fiber. Both methods are destructive. We are confident that our research makes a substantial contribution to the ongoing initiatives aimed at improving the efficiency and effectiveness of quality assessment within the beer industry.

2. Principle of operation

LPFGs and MZIs are key components in the field of optical fiber sensing technology. An LPFG operates on the principle of coupling light from a guided mode into forward propagating cladding modes (Haus and Huang, 1991). This coupling is wavelength-dependent, resulting in a spectrally selective loss. The LPFG is created by inducing periodic modulations of the refractive index and/or geometry along a single-mode optical fiber (Bock et al., 2007; Yin et al., 2014).

The transmission spectrum of an LPFG consists of a series of rejection bands at discrete resonance wavelengths. These bands are the result of the coupling of light from the fundamental core mode to co-propagating cladding modes at specific resonance wavelengths. The transmission spectrum has dips at the wavelengths corresponding to resonances with various cladding modes (Vengsarkar et al., 1996):

$$\lambda_{res}^m = (n_{eff,co} - n_{eff,cl}^m)\Lambda \quad (1)$$

where λ_{res}^m is the $-m$ th wavelength that light was coupled (resonant wavelength), $n_{eff,co}$ and $n_{eff,cl}^m$ are the core and cladding mode's effective refractive index, m denotes the cladding mode, and Λ is the grating period (generally hundreds of microns for LPFGs).

The effective index of the cladding modes of LPFGs is very sensitive to changes in the surrounding refractive index (SRI) (Jiang et al., 2022). These bands shift in response to changes in the external refractive index (RI), allowing the sensor to measure the RI of the surrounding

medium (Qi et al., 2014). When materials that absorb light at specific wavelengths are applied to the fiber, they alter the transmission characteristics, enabling absorbance measurements (Burgess, 1995). Naturally, Eq. (1) shows that should be sensitive to the SRI (Shu et al., 2002), indeed:

$$\frac{d\lambda_{res}}{dn_{sur}} = -\lambda_{res} \frac{\frac{d\lambda_{res}}{d\Lambda}}{n_{eff,co} - n_{eff,cl}^m} \frac{u_m^2 \lambda_{res}^3 n_{sur}}{8\pi r_{cl}^3 (n_{eff,co} - n_{eff,cl}^m)(n_{cl}^2 - n_{sur}^2)^{\frac{3}{2}}} \quad (2)$$

where, u_m is the zeroth-order Bessel function m th root, r_{cl} and n_{cl} is the cladding radius and refractive index, respectively. And for that matter, LPFG-based SRI probes has been extensively reported in the literature (Chen et al., 2016; Chiang et al., 2000; Gan et al., 2022; Li et al., 2011; Liu et al., 2023; Qi et al., 2014; Shen et al., 2017; Tan et al., 2014).

An optical fiber MZI, on the other hand, can present several topologies. However, a MZI is essentially an optical device that splits light into two and recombines them. When light is recombined an interference pattern emerges due to the optical path difference of different wavelengths. Consequently, an even-so-small change in the optical path, changes the interference pattern (Liao et al., 2017; Ahmed et al., 2019; Ahsani et al., 2019).

For an MZI based on two identical LPFGs, the interference occurs between the core and cladding modes. I.e., one LPFG couples light to cladding modes and a second one recouples the cladding modes to the core. The difference between the core and cladding different effective refractive index induce an optical path difference, with phase difference given by Dong et al. (2006), Lee and Nishii (1999):

$$\theta = \frac{2\pi}{\lambda} (n_{eff,co} - n_{eff,cl}^m)L \quad (3)$$

where λ is the wavelength and L is the interference length. Discarding the fiber dispersion, the distance between two adjacent minimum transmission dips at the LPFG-based MZI fringes is given by:

$$\Delta\lambda = \frac{\lambda^2}{L(n_{eff,co} - n_{eff,cl}^m)} \quad (4)$$

Hence, SRI changes impact the fringe pattern in both position and spacing. Consequently, the LPFG-base MZI results in a highly sensitive and full-of-information sensor due to the fringe variation and spectral complexity (en Fan et al., 2011; Vasconcelos et al., 2019). But these advantages can also be extrapolated to other in-fiber MZI topologies, such as LPFG-bitaper (Xue et al., 2013) and LPFG-taper (Filho et al., 2023).

The phenomena of absorbance in optical fibers, particularly in long-period fiber gratings (LPFGs), is essential for the functioning of sensors that detect changes in the refractive index and can be related to the measurement of International Bitterness Units (IBUs) in beer. When a material that absorbs light at specific wavelengths is applied to the fiber, the absorbance changes the light transmission characteristics of the LPFG (Luo and Gu, 2011; Anderson et al., 1996). This principle is similar to the method used for determining IBUs, where an acidified sample of beer is extracted with iso-octane, and the absorbance of ultraviolet light at 275 nm is measured to quantify the bitterness. The combination of high sensitivity to refractive index changes and the ability to detect specific absorbance characteristics allows optical fiber sensors to effectively measure biochemicals distinguished by their refractive index values and absorbance properties (Shakya and Singh, 2022).

3. Methods

All data used in this work, to evaluate the beer samples were obtained by the proposed sensor. The optical setup for acquiring the signals was: BP1 LED from DenseLight, the proposed optical sensor, and an Ibsen USB512 optical spectrum analyzer (OSA).

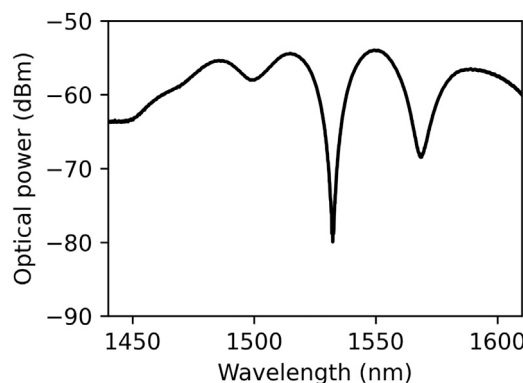


Fig. 1. Optical fiber sensor spectrum.

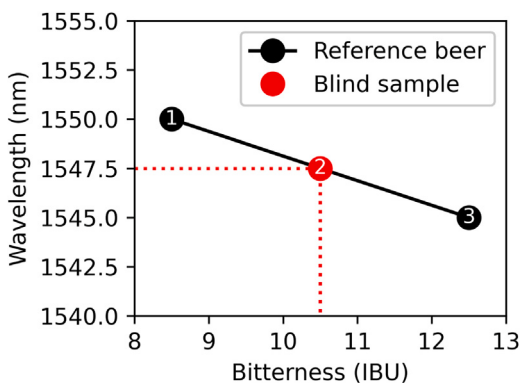


Fig. 2. Illustration of the two-point on-line self-calibrating procedure.

The optical fiber sensor was manufactured using two LPFGs, spaced by a $L = 15 \pm 1$ mm section of bare fiber. The LPFGs were arc induced (Rego, 2016) with $A = 500 \pm 1$ μm period by a fusion splicer coupled to a linear stage. During the manufacturing process, the optical spectrum was monitored using the Fourier transform OSA ThorLabs OSA203. However, due to the splicing machine arc variability and translation stage errors, no two sensors are exactly equal. Consequently, the interference pattern observed at the MZI transmission is affected. The optical fiber sensor was glued to a 3d-printed plastic support using two component epoxy, for mechanical stability, forming the sensor probe.

We used the MZI fringe positioning to measure beer bitterness. The optical spectrum obtained by the OSA was processed in real time by:

- (a) Smoothing: Savitzky–Golay zero-phase filtering;
- (b) Dip finding: we found all fringes by derivative-based local minima detection;
- (c) Resonance fitting: we fitted a modified Lorentzian function around the dips to find the dips resonant wavelength, namely λ_{rs}

The sensor spectrum, obtained after manufacturing can be seen in Fig. 1. Note that the LPFGs might have been slightly different, as the fringe pattern is not as characteristic as some MZIs reported in the literature. Even so, we were able to obtain two resonant dips within the Ibsen USB512 range, at 1530 nm and 1565 nm, hence we could monitor two wavelengths to estimate beer bitterness.

Since beer is a complex sample and its optical characteristics changes due to its varying physical-chemical parameters, we propose a relative measure of bitterness, by comparison. Hence, the sensor could be used for every beer brand and type, as long as similar samples with known bitterness are provided. Note that this approach simplifies the sensor operation and eliminates the need for calibration across different types and brands of beer. Moreover, samples with known bitterness are kept within the factory, including a standard sample for evaluating the lab measurement of bitterness.

So, our proposal uses two-point on-line self-calibrating procedure, as schematized in Fig. 2: a sample with low bitterness is presented to the sensor, then the sample under measurement, and finally a sample with high bitterness. For all three samples, we record the resonant dips and trace curves relating λ_{rs} to the bitterness. By triangulation, we were able to determine the blind sample. Moreover, this procedure was repeated for all resonant dips found within the OSA spectral range and the mean bitterness was considered.

For each beer sample, at least 50 spectra were collected per measurement. In each spectrum, the same processing technique was applied: initially, Savitzky–Golay zero-phase filtering was used to reduce noise. Then, the central wavelength λ_{rs} was identified and extracted. With the central wavelength obtained from each spectrum, boxplots calculated for each sample, providing a visual representation of the

data distribution and allowing for the identification of any outliers. After determining the summary statistics for the calibration samples (minimum bitterness, test, and maximum bitterness), a calibration curve was established through linear fitting to the average wavelength points obtained from each measurement of each sample. This calibration curve was essential for correlating the resonant wavelengths with the known bitterness levels of the calibration samples. With the established calibration curve, the bitterness of the test samples was determined by interpolating the average wavelengths obtained during the measurements.

To perform real-time data analysis and determine bitterness in the factory experiments, we developed custom software in Python. This software collected spectra directly from the OSA during each measurement, performed the filtering process, extracted the resonant wavelengths λ_{rs} , and computed summary statistics for each sample. This automated approach streamlined the analysis process in a production environment.

For the measurements, the beer sample was placed inside a glass container, we put a single drop of octanol prior to measurement to prevent bubble formation. Inside this container, we added a mini pump to keep the beer homogeneous. A plastic support holds the sensor probe inside the glass container. Between beer samples we cleaned the whole system using water-soap mixture and rinsed in water at least two times.

Fig. 3 shows the measurement apparatus, its 3d model, the manufactured sample glass container, the optical fiber probe, and a measurement example. Note that the example shown in Fig. 3(c) uses a prototype glass container without drainage, the final apparatus shown in Fig. 3(b) was used for the measurements presented in this paper.

The sensor performance was tested within two contexts: lab evaluation and factory evaluation. The main objective of lab tests was to address how the measurements varied on the same day and across days, to estimate the sensor repeatability and reproducibility. We tested 10 different beer samples, across three brands and several manufacturing lots. At the factory, with more reliable reference samples and blind sample check, we evaluated sensor bias.

In this paper we named the samples by a letter followed by a number. The letter indicates the beer brand, whereas the number its lot. For example: sample A1 is beer brand A, lot 1. We employed a total of 10 distinct samples representing 3 different beer brands and various lots. These samples were further divided into 5 replicates per day, resulting in a variable number of replicates per sample ranging from 10 (sample A) to 30 (sample B1). This variation in replicate number was due to the experimental design and resource constraints.

The validation method used to measure IBU in the samples was performed according to Bishop (1964). The procedure was divided into four main steps: solution preparation, sampling and sample preparation, analysis and results. Solution preparation began with the verification of the absorbance of iso-octane, the organic phase of the wort, at

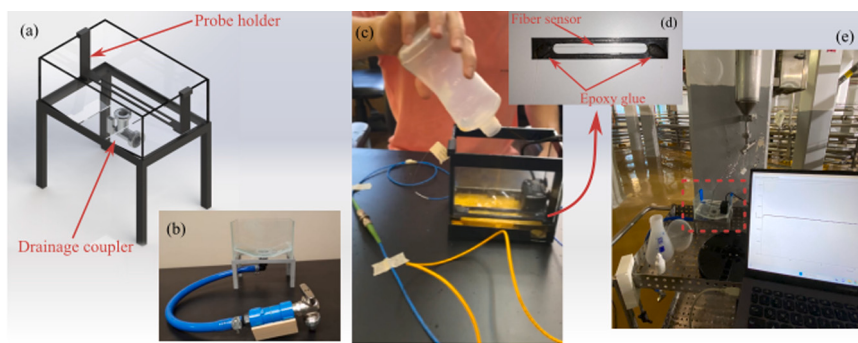


Fig. 3. Beer bitterness measurement apparatus. (a) 3D model, (b) manufactured glass container, (c) measuring example using a prototype at the lab, (d) sensor probe, and (e) measurements at the factory.

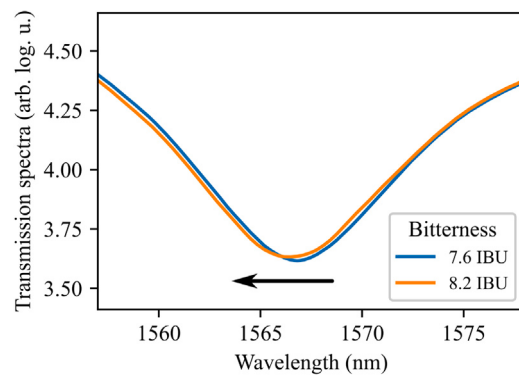


Fig. 4. Sensor response to different bitterness beers (same type and brand).

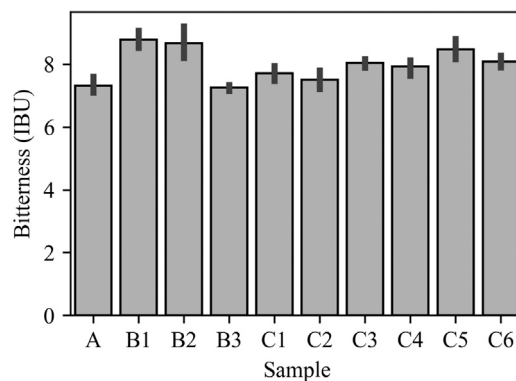


Fig. 5. Bitterness measurements for each sample using the proposed optical sensor and its bias (error bar).

275 nm. In addition to the iso-octane solution, a 3N hydrochloric acid solution was also prepared. This was prepared in an exhaust hood with controlled temperature at 20 °C. The 3N solution was made by slowly adding 250 mL of 37% (12N) *HCl* to a 1000 mL beaker containing 400 mL of distilled water under constant stirring. The solution was then transferred to a volumetric flask up to the stipulated volume and homogenized. Sample collection was carried out with the final product, just before the filling process. 1 mL of octanol was added for every 100 mL of sample and they were centrifuged at 2000 rpm for 10 min. Then the supernatant was transferred to an Erlenmeyer flask and the sample was pipetted along with 5 mL of water, followed by 1 mL of the 3N *HCl* solution and 20 mL of iso-octane. The tube was immediately closed and shaken on a horizontal shaker for 15 min, followed by centrifugation for 15 min at a minimum of 2000 rpm to separate the phases. Subsequently, the spectrophotometer was zeroed with pure iso-octane as a reference, and the absorbance of the sample was measured at 275 nm. This absorbance value was used to calculate the IBU, according to the equation for isomerized hops (5).

$$IBU = UV_{absorbance(275 \text{ nm})} * 57 * 2 \quad (5)$$

4. Results

Our results showed the resonant wavelength decreases with bitterness increments. Fig. 4 shows the 1565 nm resonant dip response for two different beer samples, note that these samples came from the same beer type and brand. The axis is the Ibsen USB512 log-scaled analog to digital converter count.

Fig. 5 shows the measurements collected with the proposed sensor at the lab, note that all data was fused together. So, we could obtain each sample bitterness and compare the estimated value with the actual sample bitterness, measured using traditional method (UV spectroscopy). The estimated bias was $-0.5 \pm 0.4 \text{ IBU}$. Note that the tests

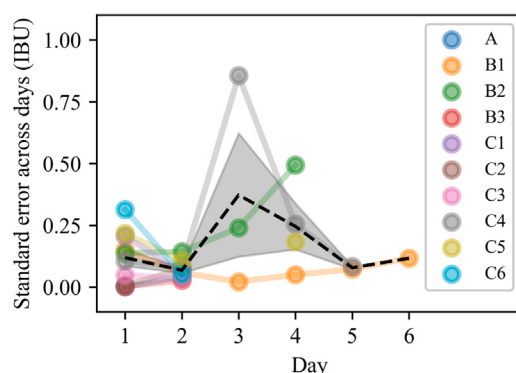


Fig. 6. Standard error of measurements for each sample across several days.

were carried among several days, so sample aging might have affected the bias evaluation as bitterness changes with aging.

The evolution of the standard error across these days, on the other hand is an interesting metric, as it provides a repeatability estimation, note that at each day the measurement conditions were the same. Fig. 6 shows the standard error for each sample among several days, with the shaded area representing the maximum and minimum variation and the dashed line showing the average variation, considering the average measurement error of all samples. We estimated sensor repeatability should not exceed 0.4IBU, considering the average of all samples measured in a day, and that the typical value is $0.17 \pm 0.09 \text{ IBU}$.

Considering the measurement for each sample, we calculated the standard error for each sample. This represents the sensor reproducibility. Despite each day having the same conditions, when we consider the standard error for each beer sample in different days, we obtain

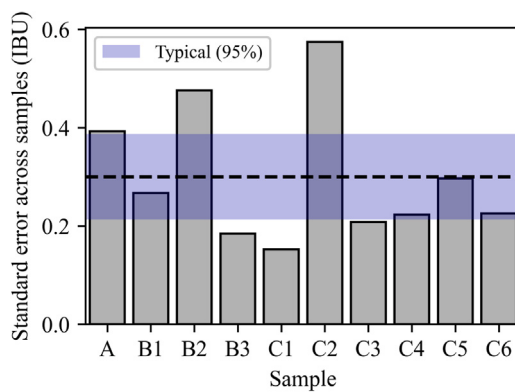


Fig. 7. Standard error of measurements for each sample, representing sensor reproducibility, with typical reproducibility estimated at 0.30 ± 0.08 IBU and a maximum of 0.57 IBU.

a measure of reproducibility. Based on the results shown in Fig. 7 we were able to estimate that the sensor reproducibility is typically 0.30 ± 0.08 IBU and should not exceed 0.57 IBU. The blue shaded area in the figure represents the 95% confidence interval for the typical standard deviation values across all samples, while the dashed line indicates the average standard deviation for all samples.

Finally, we made seven more measurements at the beer factory, each with a different sample, the measurements obtained by the proposed sensor were compared to the UV absorbance lab test, realized quasi-simultaneously, so the bias estimation could be as precise as possible. We estimate the bias as 0.1 ± 0.3 IBU.

5. Conclusion

This paper has presented a novel optical fiber sensor for measuring the bitterness of beer samples. The proposed sensor is based on a Mach-Zehnder interferometer, composed of two long-period fiber gratings. The sensor exploits the sensitivity of the LPFGs to the refractive index of the surrounding medium, which varies according to the concentration of iso- α -acids that cause bitterness in beer. The sensor uses a two-point on-line self-calibrating procedure to estimate the bitterness of unknown samples by comparison with reference samples of known bitterness.

The sensor performance was evaluated in both laboratory and factory settings, showing good repeatability, reproducibility, and low bias. We estimated the typical repeatability to be between 0.08–0.26 IBU, with typical reproducibility of 0.22–0.38 IBU, and bias within 0.2–0.4 IBU range. Which are excellent results for a portable sensor, since the proposed sensor offers a fast, simple, and low-cost alternative to the conventional method of measuring beer bitterness based on UV spectroscopy.

Future work should focus on improving the sensor robustness, encapsulation, and miniaturization.

CRediT authorship contribution statement

Renato Luiz Faraco Filho: Writing – original draft, Validation, Methodology, Investigation, Data curation, Conceptualization. **Felipe Oliveira Barino:** Writing – original draft, Visualization, Software, Methodology, Formal analysis, Data curation, Conceptualization. **João Victor Calderano:** Investigation, Data curation. **Deivid Campos:** Methodology, Investigation. **Ítalo Fernandes Valle Alvarenga:** Funding acquisition, Conceptualization. **André William Paviani Manhas:** Validation, Resources, Project administration. **Alexandre Bessa dos Santos:** Validation, Supervision, Project administration, Methodology, Funding acquisition.

Declaration of competing interest

This research was financially supported by Ambev Brewing Company. In addition to providing financial support, Ambev also supplied the beer samples used in this study and the results of conventional bitterness measurements of each sample. Despite these contributions, Ambev had no role in the development of the sensor probe, study design, data collection, and analysis. The views and interpretations expressed in this paper are solely those of the authors and do not necessarily reflect the views of Ambev Brewing Company.

Data availability

The data that has been used is confidential.

Acknowledgments

The authors would like to thank the financial support from the Coordenação de Aperfeiçoamento de Pessoal de Nível Superior (CAPES), Conselho Nacional de Desenvolvimento Científico e Tecnológico (CNPq), Fundação de Amparo à Pesquisa do Estado de Minas Gerais (FAPEMIG), Instituto Nacional de Ciência e Tecnologia em Energia Elétrica (INERGE), and Ambev.

References

- Ahmed, F., Ahsani, V., Jo, S., Bradley, C., Toyserkani, E., Jun, M.B.G., 2019. Measurement of in-fiber refractive index change using a Mach-Zehnder interferometer. *IEEE Photonics Technol. Lett.* 31, 74–77. <http://dx.doi.org/10.1109/LPT.2018.2883913>.
- Ahsani, V., Ahmed, F., Jun, M., Bradley, C., 2019. Tapered fiber-optic Mach-Zehnder interferometer for ultra-high sensitivity measurement of refractive index. *Sensors* 19, 1652. <http://dx.doi.org/10.3390/s19071652>.
- Anderson, B.B., Brodsky, A.M., Burgess, L.W., 1996. Grating light reflection spectroscopy for determination of bulk refractive index and absorbance. *Anal. Chem.* 68, 1081–1088. <http://dx.doi.org/10.1021/ac951177s>.
- Benadouda, K., Sajid, S., Chaudhri, S.F., Tazally, K.J., Nielsen, M.M.K., Prabhala, B.K., 2023. Current state of sensors and sensing systems utilized in beer analysis. *Beverages* 9, 5. <http://dx.doi.org/10.3390/beverages9010005>.
- Bishop, L.R., 1964. The measurement of bitterness in beers. *J. Inst. Brewing* 70, 489–497. <http://dx.doi.org/10.1002/j.2050-0416.1964.tb06354.x>.
- Blanco, C.A., Fuente, R.D.L., Caballero, I., Rodríguez-Méndez, M.L., 2015. Beer discrimination using a portable electronic tongue based on screen-printed electrodes. *J. Food Eng.* <http://dx.doi.org/10.1016/j.jfoodeng.2015.02.018>.
- Bock, W.J., Chen, J., Mikulic, P., Eftimov, T., 2007. A novel fiber-optic tapered long-period grating sensor for pressure monitoring. *IEEE Trans. Instrum. Meas.* 56, 1176–1180. <http://dx.doi.org/10.1109/TIM.2007.899904>.
- Burgess, L.W., 1995. Absorption-based sensors. *Sensors Actuators B* 29, 10–15. [http://dx.doi.org/10.1016/0925-4005\(95\)01657-0](http://dx.doi.org/10.1016/0925-4005(95)01657-0).
- Cañas, H., Mula, J., Díaz-Madroñero, M., Campuzano-Bolarín, F., 2021. Implementing industry 4.0 principles. *Comput. Ind. Eng.* 158, 107379. <http://dx.doi.org/10.1016/j.cie.2021.107379>.
- Chen, Y., Tang, F., Bao, Y., Tang, Y., Chen, G., 2016. A Fe-C coated long-period fiber grating sensor for corrosion-induced mass loss measurement. *Opt. Lett.* 41, 2306. <http://dx.doi.org/10.1364/OL.41.002306>.
- Chiang, K.S., Liu, Y., Ng, M.N., Dong, X., 2000. Analysis of etched long-period fibre grating and its response to external refractive index. *Electron. Lett.* 36, 966. <http://dx.doi.org/10.1049/el:20000701>.
- Damerow, P., 2012. Sumerian beer: the origins of brewing technology in ancient mesopotamia. *Cuneif. Digit. Libr. J.* 2012, URL <https://cdli.mpiwg-berlin.mpg.de/articles/cdlj/2012-2>.
- Dong, X., Su, L., Shum, P., Chung, Y., Chan, C.C., 2006. Wavelength-selective all-fiber filter based on a single long-period fiber grating and a misaligned splicing point. *J. Food Eng.* <http://dx.doi.org/10.1016/j.joptcom.2005.07.075>, URL www.elsevier.com/locate/joptcom.
- Esmaily, R., Razavi, M.A., Razavi, S.H., 2024. A step forward in food science, technology and industry using artificial intelligence. *Trends Food Sci. Technol.* 143, 104286. <http://dx.doi.org/10.1016/j.tifs.2023.104286>.
- en Fan, Y., Zhu, T., Shi, L., Rao, Y.-J., 2011. Highly sensitive refractive index sensor based on two cascaded special long-period fiber gratings with rotary refractive index modulation. *Appl. Opt.* 50, 4604. <http://dx.doi.org/10.1364/AO.50.004604>.
- Filho, R.L.F., Barino, F.O., Calderano, J., Alvarenga, I.F.V., Campos, D., dos Santos, A.B., 2023. In-fiber Mach-Zehnder interferometer as a promising tool for optical nose and odor prediction during the fermentation process. *Opt. Lett.* 48, 3905. <http://dx.doi.org/10.1364/OL.486742>.

- Filho, R.L.F., dos Santos, A.B., Barbero, A.P.L., Silva, V.N.H., 2021. Optical inclinometer based on a LPG-taper series configuration. *J. Microw. Optoelectron. Electromagn. Appl.* 20, 612–620. <http://dx.doi.org/10.1590/2179-10742021v20i3254754>.
- Gan, W., Li, Y., Liu, T., Yang, Y., Song, B., Dai, S., Xu, T., Wang, Y., Lin, T.-J., Zhang, P., 2022. Rapid and sensitive detection of ammonia in water by a long period fiber grating sensor coated with sol-gel silica. *Opt. Express* 30, 33817. <http://dx.doi.org/10.1364/OE.472205>.
- Hassoun, A., Jagtap, S., Garcia-Garcia, G., Trollman, H., Pateiro, M., Lorenzo, J.M., Trif, M., Rusu, A.V., Aadil, R.M., Simat, V., Cropotova, J., Câmara, J.S., 2023b. Food quality 4.0: From traditional approaches to digitalized automated analysis. *J. Food Eng.* 337, 111216. <http://dx.doi.org/10.1016/j.jfoodeng.2022.111216>.
- Hassoun, A., Jagtap, S., Trollman, H., Garcia-Garcia, G., Abdullah, N.A., Goksen, G., Bader, F., Ozogul, F., Barba, F.J., Cropotova, J., Munekata, P.E., Lorenzo, J.M., 2023a. Food processing 4.0: Current and future developments spurred by the fourth industrial revolution. *Food Control* 145, 109507. <http://dx.doi.org/10.1016/j.foodcont.2022.109507>.
- Haus, H., Huang, W., 1991. Coupled-mode theory. *Proc. IEEE* 79, 1505–1518. <http://dx.doi.org/10.1109/5.104225>, URL <http://ieeexplore.ieee.org/document/104225/>.
- Hunter, R.A., Domkowski, E.J., 2018. Quantifying beer bitterness: an investigation of the impact of sample preparation. *J. Chem. Educ.* 95, 2009–2012. <http://dx.doi.org/10.1021/acs.jchemed.8b00420>.
- Jaywant, S.A., Singh, H., Arif, K.M., 2022. Sensors and instruments for brix measurement: a review. *Sensors* 22, 2290. <http://dx.doi.org/10.3390/s22062290>.
- Jiang, H., Gu, Z., Wu, J., 2022. Design of high sensitivity refractive index sensor based on small chirp coefficient LPFG. *Opt. Quantum Electron.* 54, 343. <http://dx.doi.org/10.1007/s11082-022-03747-z>.
- Lasi, H., Fettke, P., Kemper, H.-G., Feld, T., Hoffmann, M., 2014. Industrie 4.0. *Wirtschaftsinformatik* 56, 261–264. <http://dx.doi.org/10.1007/s11576-014-0424-4>.
- Lee, B.H., Nishii, J., 1999. Dependence of fringe spacing on the grating separation in a long-period fiber grating pair. *Appl. Opt.* 38, 3450. <http://dx.doi.org/10.1364/AO.38.003450>.
- Li, B., Jiang, L., Wang, S., Tsai, H.-L., Xiao, H., 2011. Femtosecond laser fabrication of long period fiber gratings and applications in refractive index sensing. *Opt. Laser Technol.* 43, 1420–1423. <http://dx.doi.org/10.1016/j.optlastec.2011.04.011>.
- Liao, H., Lu, P., Fu, X., Jiang, X., Ni, W., Liu, D., Zhang, J., 2017. Sensitivity amplification of fiber-optic in-line Mach-Zehnder interferometer sensors with modified vernier-effect. *Opt. Express* 25, 26898. <http://dx.doi.org/10.1364/OE.25.026898>.
- Liu, T., Li, Y., Dai, X., Gan, W., Wang, X., Dai, S., Song, B., Xu, T., Zhang, P., 2023. Simultaneous detection of temperature, strain, refractive index, and pH based on a phase-shifted long-period fiber grating. *J. Lightwave Technol.* 41, 5169–5180. <http://dx.doi.org/10.1109/JLT.2023.3254550>.
- Luo, T., Gu, Z.-T., 2011. A new type of absorbance sensors based on long-period fiber gratings. *Chin. Phys. Lett.* 28, 054207. <http://dx.doi.org/10.1088/0256-307X/28/5/054207>.
- Qi, L., Zhao, C.-L., Yuan, J., Ye, M., Wang, J., Zhang, Z., Jin, S., 2014. Highly reflective long period fiber grating sensor and its application in refractive index sensing. *Sensors Actuators B* 193, 185–189. <http://dx.doi.org/10.1016/j.snb.2013.11.063>.
- Rego, G., 2016. Arc-induced long period fiber gratings. *J. Sens.* 2016, 1–14. <http://dx.doi.org/10.1155/2016/3598634>, URL <http://www.hindawi.com/journals/js/2016/3598634/>.
- Roriz, P., Silva, S., Frazão, O., Novais, S., 2020. Optical fiber temperature sensors and their biomedical applications. *Sensors* 20, 2113. <http://dx.doi.org/10.3390/s20072113>.
- Shakya, A.K., Singh, S., 2022. Design of biochemical biosensor based on transmission, absorbance and refractive index. *Biosens. Bioelectron.* 180, 100089. <http://dx.doi.org/10.1016/j.bios.2021.100089>.
- Shen, F., Wang, C., Sun, Z., Zhou, K., Zhang, L., Shu, X., 2017. Small-period long-period fiber grating with improved refractive index sensitivity and dual-parameter sensing ability. *Opt. Lett.* 42, 199. <http://dx.doi.org/10.1364/OL.42.000199>.
- Shi, Y., Gong, F., Wang, M., Liu, J., Wu, Y., Men, H., 2019. A deep feature mining method of electronic nose sensor data for identifying beer olfactory information. *J. Food Eng.* <http://dx.doi.org/10.1016/j.jfoodeng.2019.07.023>.
- Shu, X., Zhang, L., Bennion, I., Shu, X., Zhang, L., Bennion, I., Shu, X., Zhang, L., Bennion, I., 2002. Sensitivity characteristics of long-period fiber gratings. *J. Lightwave Technol.* 20, 255–266. <http://dx.doi.org/10.1109/50.983240>, URL <http://ieeexplore.ieee.org/document/983240/>.
- Tan, Y., Ji, W., Mamidala, V., Chow, K., Tjin, S., 2014. Carbon-nanotube-deposited long period fiber grating for continuous refractive index sensor applications. *Sensors Actuators B* 196, 260–264. <http://dx.doi.org/10.1016/j.snb.2014.01.063>.
- Tsai, Y.-C., Huang, J.-D., Chiu, C.-C., 2007. Amperometric ethanol biosensor based on poly(vinyl alcohol)-multiwalled carbon nanotube-alcohol dehydrogenase biocomposite. *Biosens. Bioelectron.* 22, 3051–3056. <http://dx.doi.org/10.1016/jbios.2007.01.005>.
- Vasconcelos, H.C.A.S.G., de Almeida, J.M.M.M., Saraiva, C.M.T., da Silva Jorge, P.A., Coelho, L.C.C., 2019. Mach-Zehnder interferometers based on long period fiber grating coated with titanium dioxide for refractive index sensing. *J. Lightwave Technol.* 37, 4584–4589. <http://dx.doi.org/10.1109/JLT.2019.2912829>, URL <https://ieeexplore.ieee.org/document/8695793/>.
- Vengsarkar, A.M., Lemaire, P.J., Judkins, J.B., Bhatia, V., Erdogan, T., Sipe, J.E., 1996. Long-period fiber gratings as band-rejection filters. *J. Lightwave Technol.* 14, 58–65.
- Viejo, C.G., Fuentes, S., 2020. Low-cost methods to assess beer quality using artificial intelligence involving robotics, an electronic nose, and machine learning. *Fermentation* 6, 104. <http://dx.doi.org/10.3390/fermentation6040104>.
- Xu, Z., Luo, Y., Mao, Y., Peng, R., Chen, J., Soteyome, T., Bai, C., Chen, L., Liang, Y., Su, J., Wang, K., Liu, J., Kjellerup, B.V., 2020. Spoilage lactic acid bacteria in the brewing industry. *J. Microbiol. Biotechnol.* 30, 955–961. <http://dx.doi.org/10.4014/jmb.1908.08069>.
- Xue, X., Zhang, W., Zhang, H., Gao, S., Geng, P., Bai, Z., Li, J., 2013. Simultaneous measurement of temperature and refractive index using a simplified modal interferometer composed of tilted long-period fiber grating and fiber bitaper. *Meas. Sci. Technol.* 24, 065103. <http://dx.doi.org/10.1088/0957-0233/24/6/065103>.
- Yin, G., Wang, Y., Liao, C., Zhou, J., Zhong, X., Wang, G., Sun, B., He, J., 2014. Long period fiber gratings inscribed by periodically tapering a fiber. *IEEE Photonics Technol. Lett.* 26, 698–701. <http://dx.doi.org/10.1109/LPT.2014.2302901>.
- Zhou, K., Liu, T., Zhou, L., 2015. Industry 4.0: Towards future industrial opportunities and challenges. In: 2015 12th International Conference on Fuzzy Systems and Knowledge Discovery. FSKD, IEEE, pp. 2147–2152. <http://dx.doi.org/10.1109/FSKD.2015.7382284>.